Supplementary Figure 1.

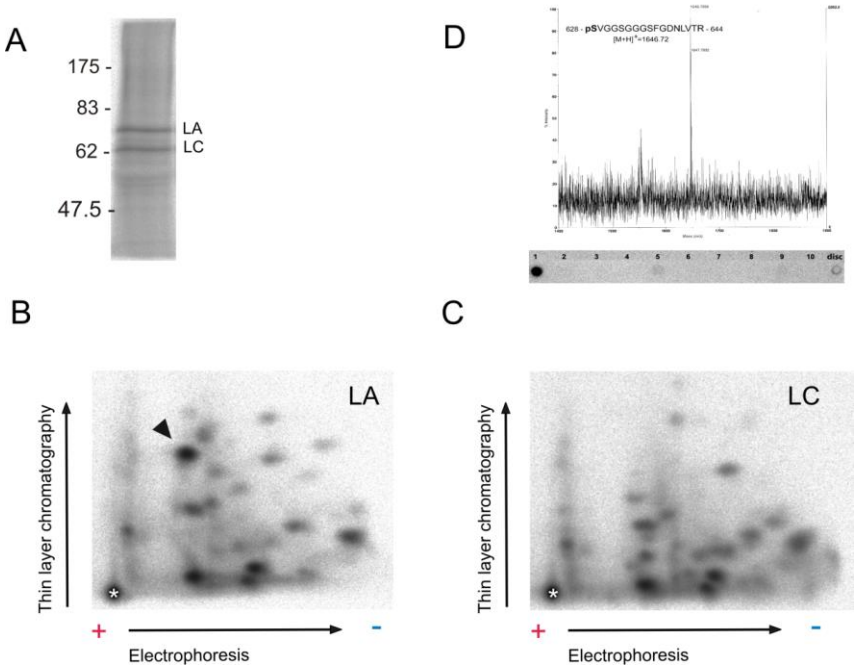

Supplementary Figure 1. SDS-PAGE and 2-D-PPM of *in vivo* phosphorylated lamins A and C, and identification of the phosphorylation sites. **(A)** The autoradiograph shows SDS-PAGE separated LA/C immunoprecipitated from HeLa cells subjected to ^{32}P-labeling. Two distinct bands of 70 and 65 kDa correspond to ^{32}P-labeled LA and LC. Tryptic phosphopeptide maps of the corresponding LA and LC bands are shown in **(B)** and **(C)** (directions of electrophoresis and ascending chromatography are indicated; sample application spot is marked with an asterisk *). Tryptic peptide maps demonstrate the overall number of individual phosphorylation sites and demonstrate marked differences between their relative stoichiometries. LA and LC maps look identical, with the exception of phosphopeptides arising from the far C-terminus, which is not present in LC due to alternative splicing. The arrow in the LA autoradiograph points to the most prominent of these far C-terminal peptides, identified **(D)** by MALDI-TOF mass spectrometry and manual Edman degradation (cycle numbers below the mass spectrum, ^{32}P release on the first cycle) as Ser-628, one of the major high turnover sites (Edman degradation shows faint label release at cycle 5, suggesting some phosphorylation at Ser-632 as well). There are more than 20 individual peptide spots on the LA map, which corresponds well to the 24 phosphopeptides identified by LC-MS/MS. (Table 1, Supplementary Fig. 2).The most prominent sites identified by MS-analysis and manual Edman degradation (data not shown) were also shown to be the most prominent in the MS-based estimation of occupancy rate of phosphorylation sites (Supplementary Fig. 2C). For the above

analyses in vivo ^{32}P labeling, Edman sequencing and mass spectrometry were performed essentially as previously described (Eriksson et al., 1998; Kochin et al., 2006). Briefly, HeLa cells were grown in DMEM (Sigma-Aldrich) supplemented with 10% serum, L-glutamine, and antibiotics. Cells at 80% confluency in 10 cm cell culture dishes were covered with 6 ml of phosphate-free minimum essential medium Eagle (MEME; Sigma-Aldrich) supplemented with 10% fetal bovine serum and containing 0.3 mCi/ml ^{32}P-orthophosphate, and incubated for 2.5 h at 37^{0}C. After an additional incubation for 30 min in the presence of 50 nM of the phosphatase inhibitor calyculin A (Sigma-Aldrich), cells were collected by centrifugation and washed with ice-cold PBS, followed by lysis in SDS-buffer. The lysate was boiled 5 min and sonicated for 20 sec with a probe sonicator. Polyclonal rabbit anti-LA/C (no. 266; Goldman laboratory) and protein A-sepharose beads (Amersham Biosciences) were used to immunoprecipitate LA/C. The phosphorylation stoichiometry of individual phosphopeptides in LA/C tryptic peptide maps was estimated by measuring and comparing photostimulated luminescence levels of individual spots. The following peptide identification by mass-spectrometry and manual Edman degradation was done exactly as previously described (Eriksson et al., 1998; Kochin et al., 2006).

Supplementary Figure 2.

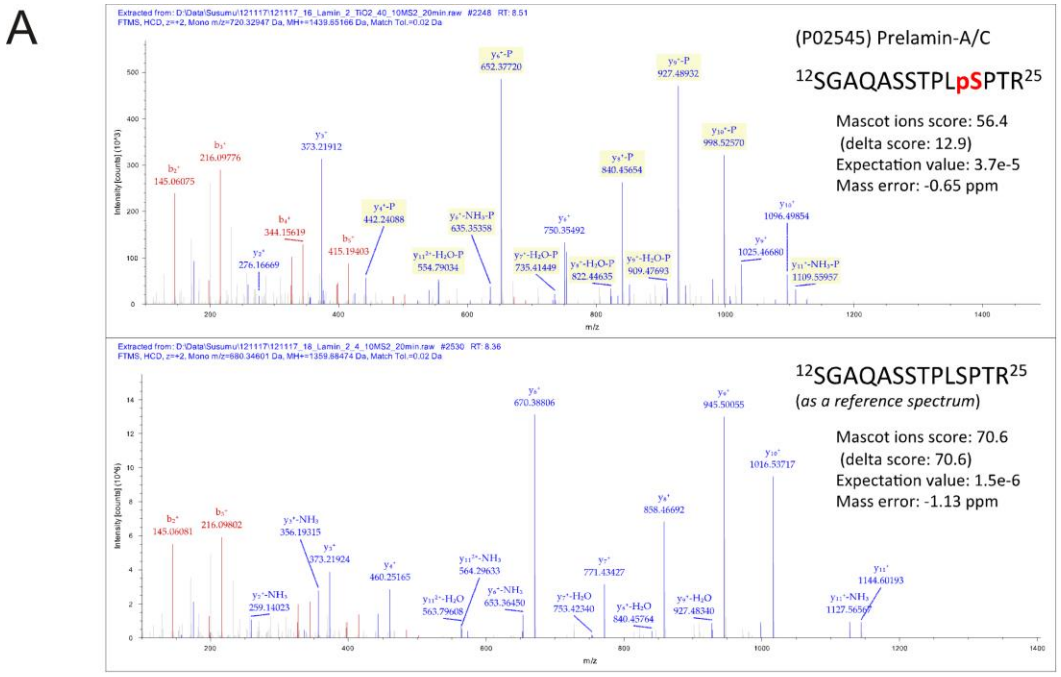

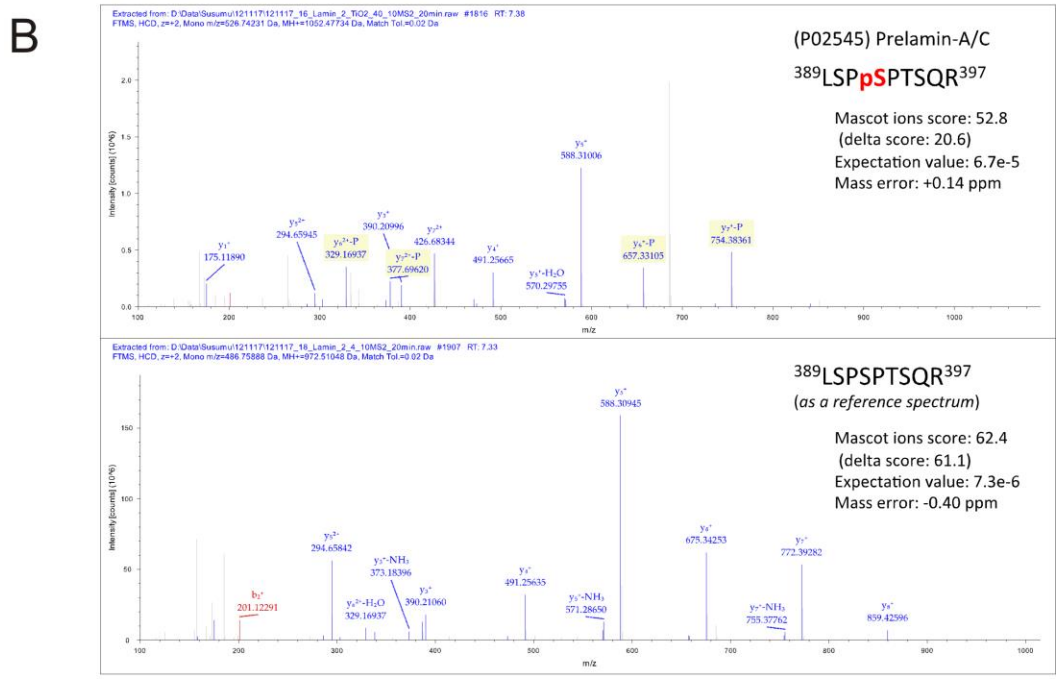

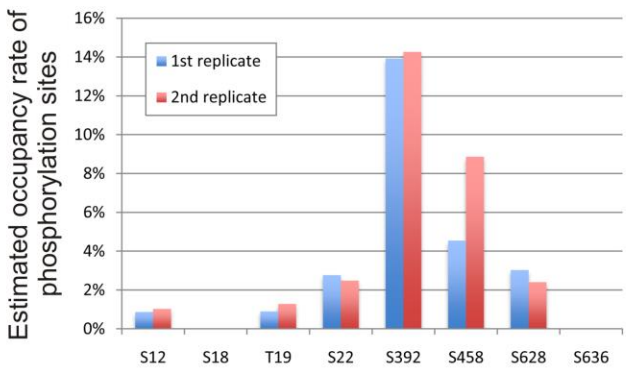

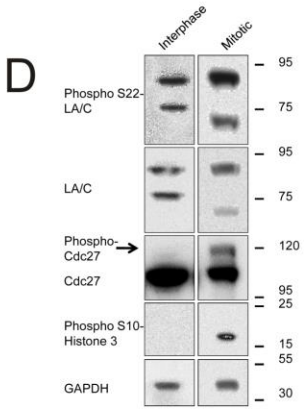

Supplementary Figure 2. (A-B) Representative MS/MS spectra of interphase LA/C phosphopeptides show phosphorylation of Ser-22 and Ser-392. After phosphopeptide enrichment by TiO_2 affinity chromatography, LC-MS/MS analysis identified LA/C phosphorylation sites, **(A)** Ser-22 and **(B)** Ser-392. Non-phosphorylated forms of the peptides identified in the non-enriched samples were used as reference peptides, and their MS/MS spectra were compared to further validate the identification of the phosphorylation sites. Also see Table 1 for other phosphorylation sites identified (see Materials and Methods in the main text). **(C)** When a phosphopeptide and its non-phosphorylated form were observed with the same charge and oxidation states in the non-enriched samples, a phosphorylation site occupancy rate was estimated based on relative peptide abundance. The occupancy rate was calculated as follows: PT / (N + PI) where PT is summed abundance of phosphopeptides containing a target phosphorylation site, N is abundance of the non-phosphorylated peptide, and PI is summed abundance of all phosphopeptide isoforms. Note, this is an approximate estimation, since phosphorylation may influence ionization efficiency and thus signal of peptides. **(D)** Western blot of mitotic markers from interphase cells. Phospho-S22 LA/C could be detected in the interphase sample (without calyculin A treatment), but, as expected, at a lower level than in the mitotic cells. The amount of mitotic markers phospho-S10 histone 3 and phospho-cdc27 are below the detection limit in interphase cells, whereas the mitotic shake off fraction, used as a positive control, show a clear band of phosphorylated cdc27 (arrow) and phospho-S10 histone 3. Mitotic cells were collected by shake off, the remaining cells were regarded as interphase cells. The cells were lysed in SDS-sample buffer, boiled at 95°C for 5 min, and the yielded protein sample was separated by SDS-PAGE on 7-12% gradient gels (Life technologies), transferred to nitrocellulose membrane, and blotted with antibodies against phospo- S22 LA/C (Cell Signaling), LA/C (Cell Signaling), Cdc27 (BD Biosciences), phospho-S10 histone 3 (Abcam) and GAPDH (Cell Signaling), for detection HRP-conjugated anti mouse (GE Healtcare) and anti rabbit (Promega) secondary antibodies were used. The images show non-adjacent lanes from the same gel and are from the same exposure.

Supplementary Figure 3.

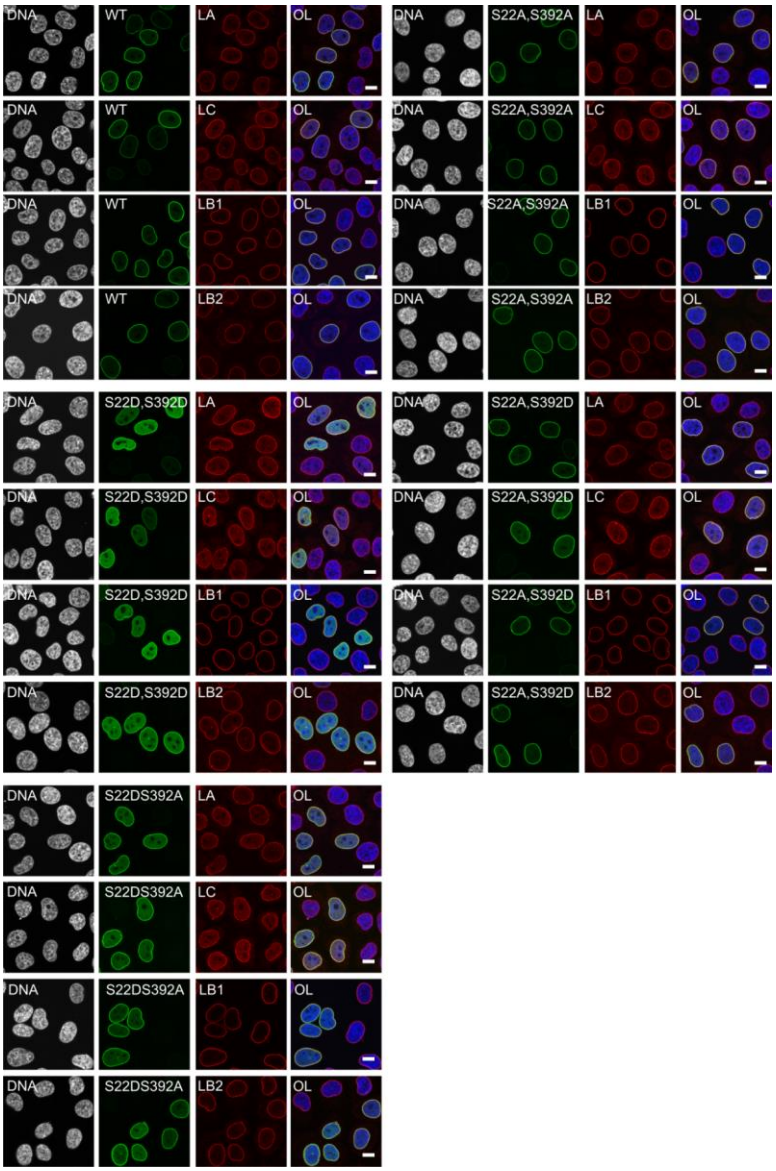

Supplementary Figure 3. Immunofluorescence analysis of the effects of phosphorylation-deficient and phospho-mimetic amino acid substitutions in LA on endogenous LA/C, LB1 and LB2 networks. Neitherphospho-mimetic nor phosphorylation-deficient substitutions at Ser-22 or Ser-392 had any effect on B-type lamin distribution. Materials and methods have been described in the main text.

Supplementary Figure 4.

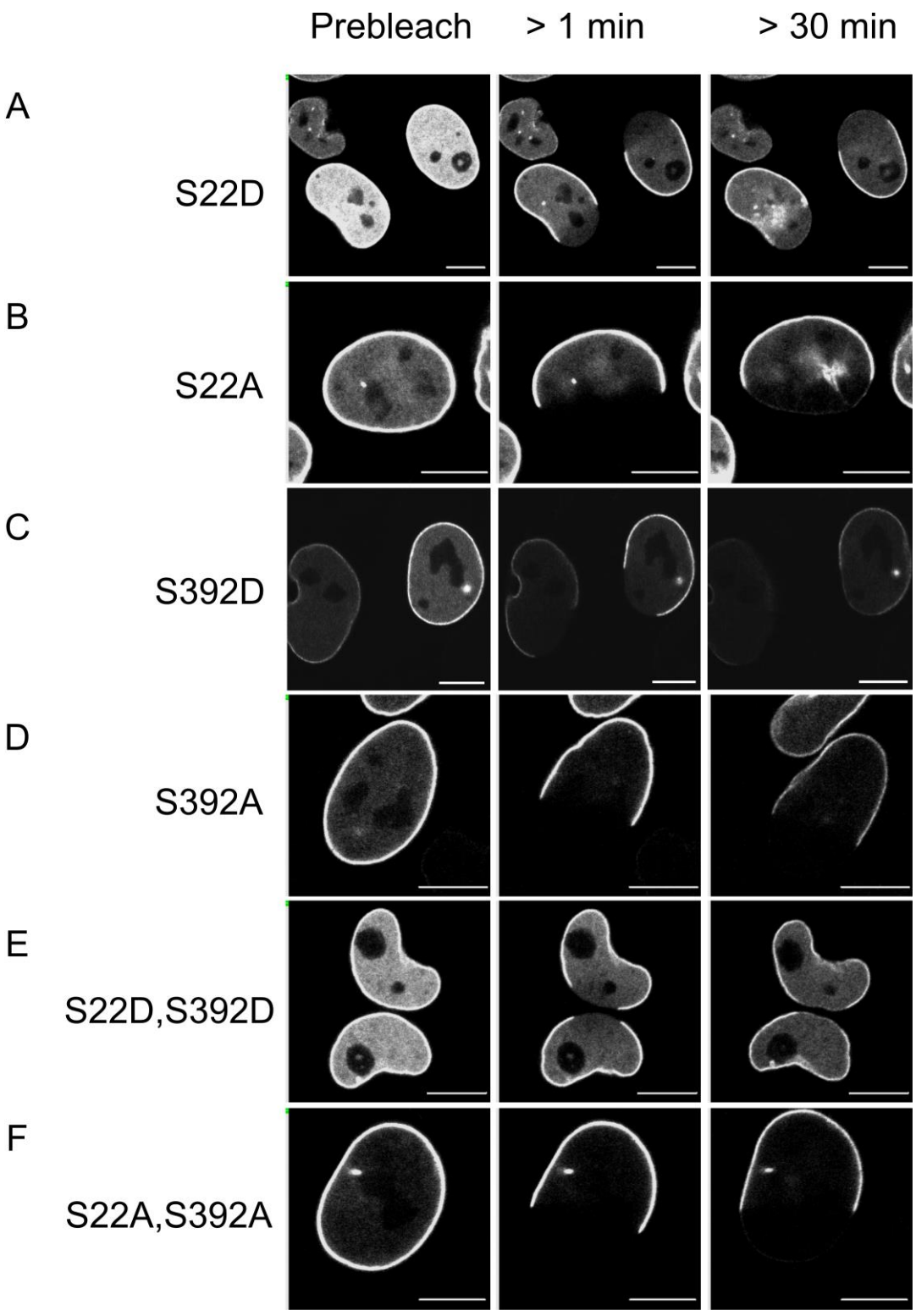

Supplementary Figure 4. FRAP analysis of nucleoplasmic LA reveals the individual roles of Ser-22 and Ser-392 in regulating nucleoplasmic LA distribution and dynamics. These results suggest that Ser-392 contributes markedly to nucleoplasmic LA dynamics; although Ser-22 also has profound effects on this fraction.